The stress dependence of the change in sound velocity in Sb-doped Ge

T Umebayashi and K Suzuki

Department of Electrical Engineering, Waseda University, Shinjuku, Tokyo 169, Japan

Abstract. We have measured the stress dependence of the change in sound velocity for Sb-doped Ge over a concentration N range 1.1×10^{16}–1.3×10^{18} cm^{-3} and a temperature range 2.3–4.2 K. The revised density of states for $N > 10^{17}$ cm^{-3} has been derived from fitting to the temperature dependence of the change in sound velocity under zero stress. Qualitative agreement is obtained between the calculation of the stress dependence using the density of states derived and the experiment.

1. Introduction

The electron–phonon interaction affects the elastic constants in doped semiconductors (see, e.g., Keyes (1968)). Therefore ultrasonic measurements are useful for studying the low-lying electronic states of doped semiconductors. In previous papers (Kohno *et al* 1988, hereafter referred to as I, Asano *et al* 1988), the temperature and the magnetic field dependences of the change in sound velocity in Sb-doped Ge over a wide concentration range have been reported. It has been found that the dependence changes with the Sb concentration, reflecting the variation in the electronic states with changing concentration and that the metal–non-metal transition in the Ge:Sb system occurs in the impurity band.

In this paper we report the results of measurements on the stress dependence of the change in sound velocity in Sb-doped Ge. Some results have been given previously in I and in the paper by Umebayashi *et al* (1989). Furthermore the revised forms are given of the density of states obtained from fitting to the temperature dependence of the change in sound velocity under zero stress, which are used in calculating the stress dependence.

2. Experimental details

The Sb-doped Ge samples used in measurements are the same as in I except for one sample with a carrier concentration of 1.1×10^{16} cm^{-3}. The carrier concentration N of the samples at room temperature is in the range 1.1×10^{16}–1.3×10^{18} cm^{-3} where the critical concentration N_c for the metal–non-metal transition is about 1.5×10^{17} cm^{-3}.

The change Δv in sound velocity has been measured using the usual pulse echo overlap method with 60 MHz longitudinal waves propagating along the [111] or [110] direction under a unixial compressional stress X of magnitude X up to 3×10^8 dyn cm^{-2} in the temperature range 2.3–4.2 K. The direction of X was perpendicular to that of the sound wave propagation, namely $X \parallel [111]$ for $q \parallel [1\bar{1}0]$ (case A) and $X \parallel [110]$ for $q \parallel [1\bar{1}1]$ (case

B) where q is the phonon wavevector. The sound waves were generated by means of a ZnO thin-film transducer grown on one face of the sample by the RF sputtering method.
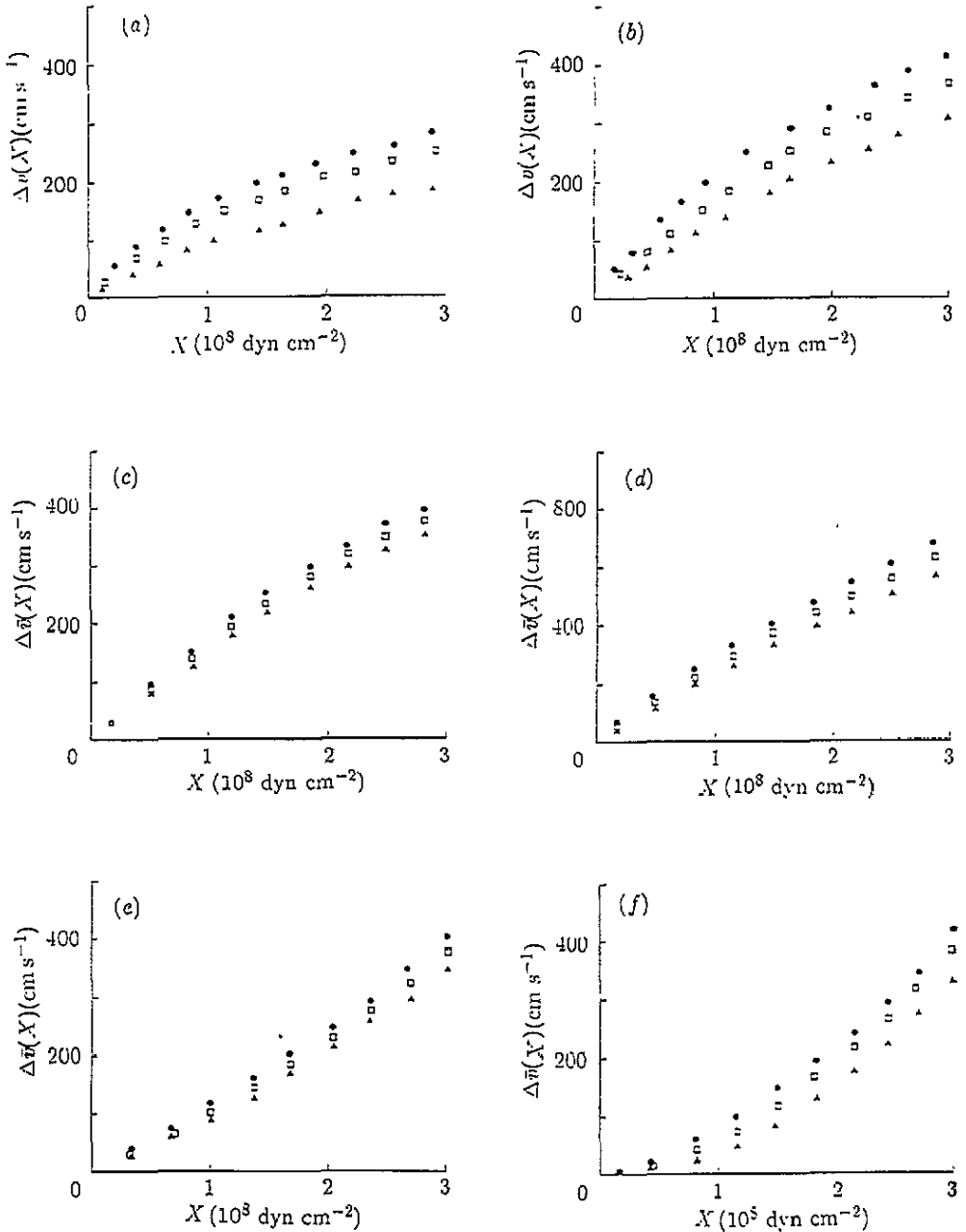
Figure 1. The dependence $\Delta\bar{v}(X)$ ($\equiv \Delta v(X) - \Delta v(0)$) of the change $\Delta\bar{v}$ in sound velocity on the stress X at $T = 2.3$ K ($\bullet$), 3.0 K ($\square$) and 4.2 K ($\blacktriangle$) for (b), (c), (e), (f) case A ($X \parallel [111]$; $q \parallel [1\bar{1}0]$) and (a), (d), (g), (h) case B ($X \parallel [110]$; $q \parallel [1\bar{1}1]$) at various concentrations N: (a) 1.1×10^{16} cm^{-3}; (b) 3.1×10^{16} cm^{-3}; (c) 1.1×10^{17} cm^{-3}; (d) 1.3×10^{17} cm^{-3}; (e) 1.6×10^{17} cm^{-3}; (f) 1.8×10^{17} cm^{-3}; (g) 4.6×10^{17} cm^{-3}; (h) 1.3×10^{18} cm^{-3}.
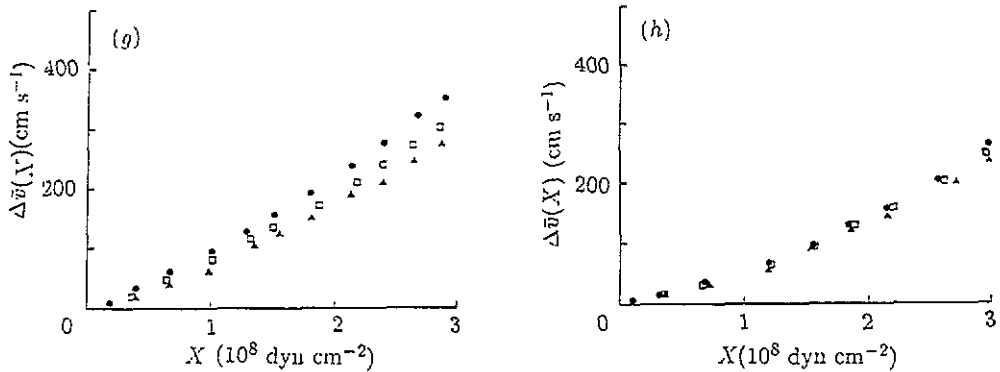
Figure 1. (Continued)

3. Results

Figure 1 shows $\Delta \bar{v}(X)$ ($\equiv \Delta v(X) - \Delta v(0)$) for $N = 1.1 \times 10^{16}$, 3.1×10^{16}, 1.1×10^{17}, 1.3×10^{17}, 1.6×10^{17}, 1.8×10^{17}, 4.6×10^{17} and 1.3×10^{18} cm^{-3} at $T = 2.3$, 3.0 and 4.2 K for case A ($X \| [111]$; $q \| [1\bar{1}0]$) and case B ($X \| [110]$; $q \| [1\bar{1}1]$). $\Delta \bar{v}(X)$ for 1.0×10^{17} cm^{-3} in case B is almost the same as for 1.1×10^{17} cm^{-3}.

The following should be pointed out. Each experimental point in figure 1 is the average of three measurements. There exists non-uniformity of strains in samples under the external stresses. The degree of non-uniformity may vary from sample to sample.

The $\Delta \bar{v}(X)$ results for $N = 1.1 \times 10^{16}$ and 3.1×10^{16} cm^{-3} have already been discussed in detail (Umebayashi *et al* 1989) where the sound waves interact with localized electrons bound to isolated donors and donor pairs. Therefore we shall not discuss them further here.

$\Delta \bar{v}(X)$ for 1.1×10^{17} and 1.6×10^{17} cm^{-3} in case B have been given in I. It has been found that $\Delta \bar{v}(X)$ is larger for case B than for case A when the concentrations are the same.

4. Discussion

4.1. General remarks

The conduction band of Ge has four equivalent valleys along the $[111]$, $[1\bar{1}\bar{1}]$, $[\bar{1}1\bar{1}]$ and $[\bar{1}\bar{1}1]$ directions in the first Brillouin zone which are denoted by valley indices 1, 2, 3 and 4, respectively. The uniaxial stresses X except for those along the $[100]$ crystallographic axes destroy the equivalence of the four valleys.

For $X \| [111]$, the change $E^{(j)}$ in energy of the bottom of the jth valley is as follows (Fritzsche 1962):

$$\Delta E^{(1)} = -\Xi_u X / 3 C_{44}$$
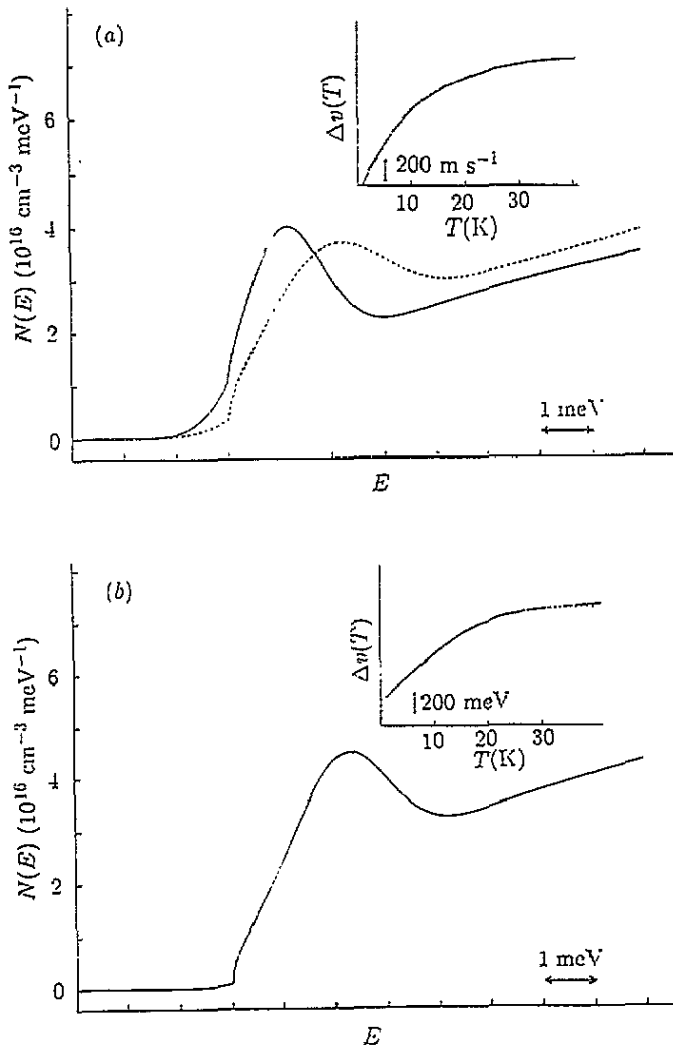$$\Delta E^{(2)} = \Delta E^{(3)} = \Delta E^{(4)} = \Xi_u X / 9 C_{44}$$

(1)

Figure 2. The density $N(E)$ of states per valley for various concentrations N: (*a*) 1.3×10^{17} cm^{-3}; (*b*) 1.8×10^{17} cm^{-3}; (*c*) 3.3×10^{17} cm^{-3}; (*d*) 4.6×10^{17} cm^{-3}; (*e*) 1.3×10^{18} cm^{-3}. The insets show the temperature dependence $\Delta v(T)$ of the change in sound velocity under zero stress: ——, calculated curves; ●, experimental data. In (*a*) the broken curve represents $N(E)$ for the case when a fraction of electrons have the same electron–phonon coupling as isolated donors (see text). In (*e*) the dotted curve represents $N(E)$ obtained from the fitting given by the broken curve in the inset.

and, for $X \parallel [110]$ (Fritzsche 1960)

$$\Delta E^{(1)} = \Delta E^{(4)} = -\Xi_u X/6C_{44}$$
$$\Delta E^{(2)} = \Delta E^{(3)} = \Xi_u X/6C_{44}$$

(2)

where $\Xi_u = 16$ eV is the shear deformation potential, $C_{44} = 0.684 \times 10^{12}$ dyn cm^{-2} is the
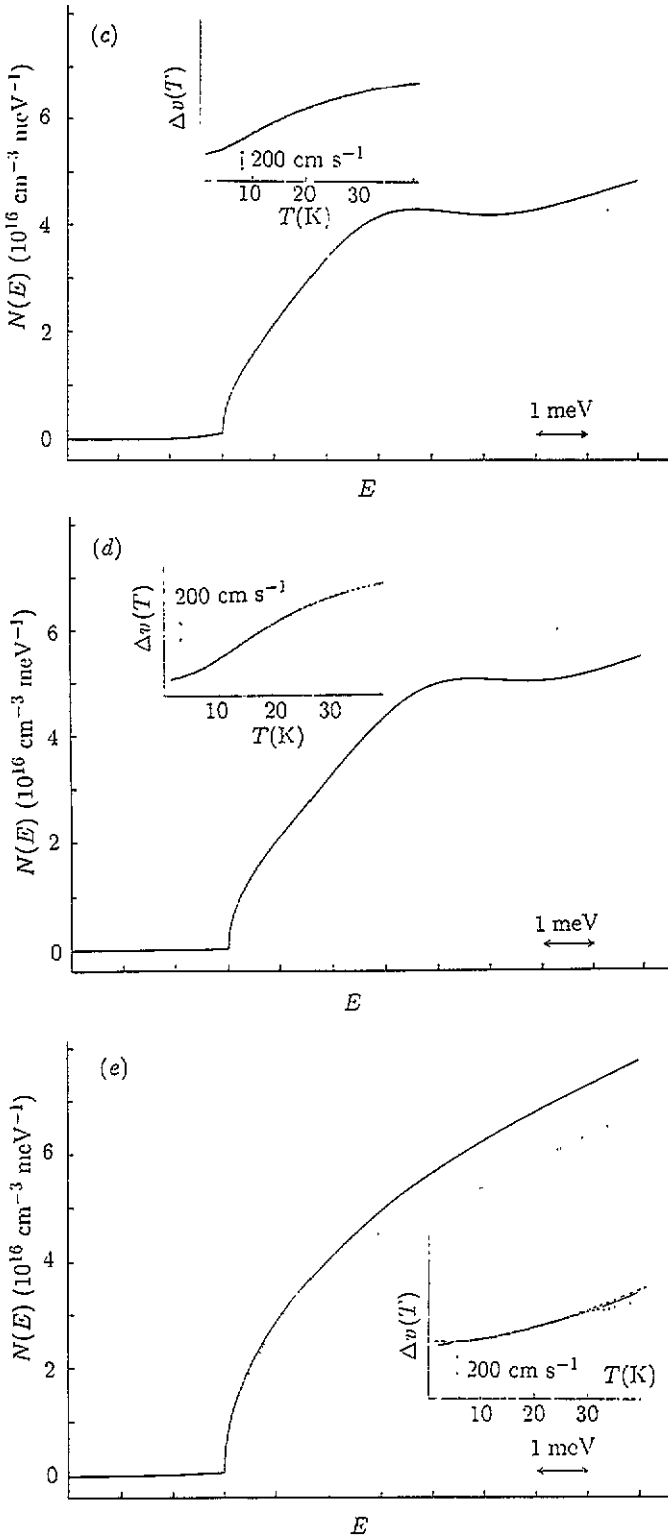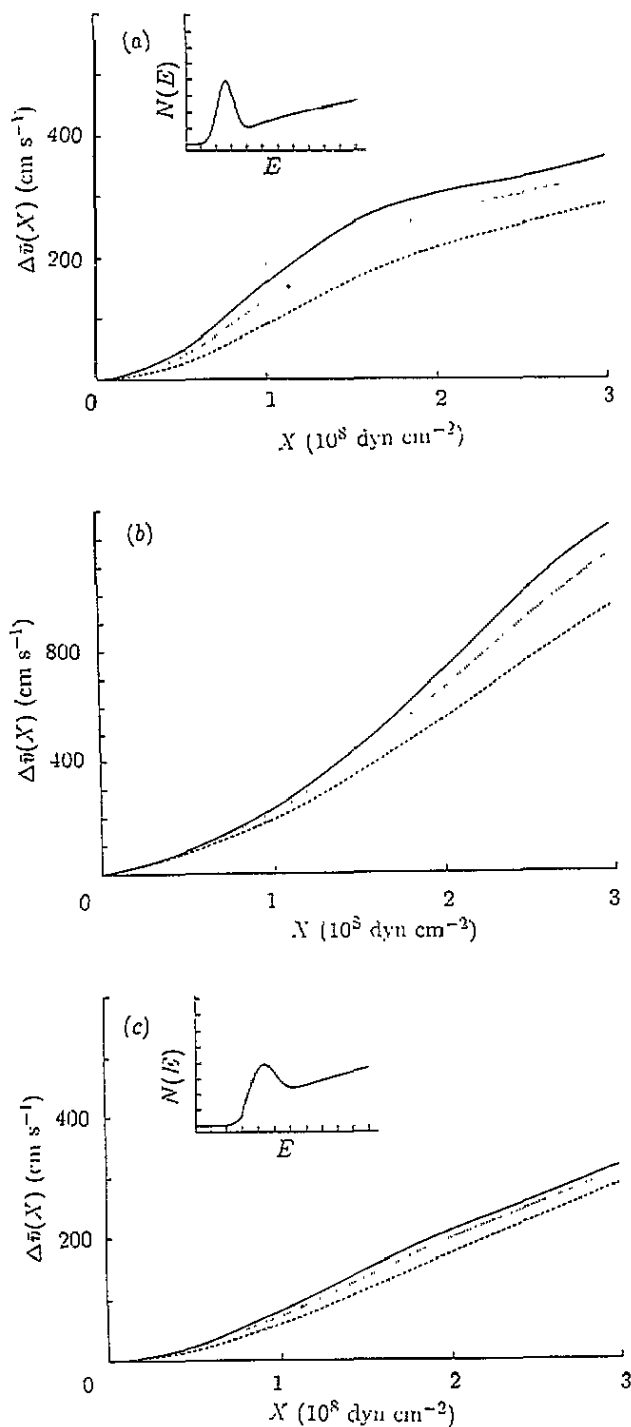
Figure 2. (Continued)

Figure 3. The calculated $\Delta\bar{v}(X)$ at $T = 2.3$ K (——), 3.0 K (·····) 4.2 K (– – –) for (*a*), (*c*), (*d*) case A and (*b*), (*e*) case B at various concentrations N: (*a*) 1.1×10^{17} cm^{-3}; (*b*) 1.3×10^{17} cm^{-3}; (*c*) 1.6×10^{17} cm^{-3}; (*d*) 1.8×10^{17} cm^{-3}; (*e*) 4.6×10^{17} cm^{-3} and 1.3×10^{18} cm^{-3}. The insets in (*a*) and (*c*) show $N(E)$ under zero stress where the scale on the axes of ordinate and abscissa is the same as that in figure 2.
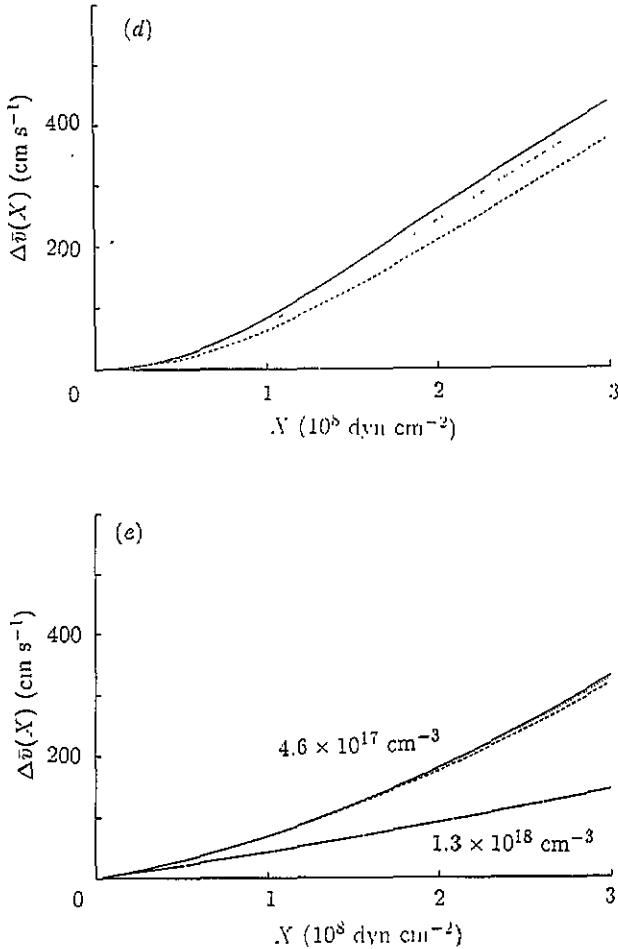
Figure 3. (Continued)

elastic stiffness constant and $X > 0$ for compression and $X < 0$ for tension.

The coupling between the sound waves and the electrons depends on the valley (see, e.g., Sota and Suzuki (1982)). For the $[1\bar{1}0]$ longitudinal waves, the strengths of the electron–phonon coupling in the four valleys are the same. On the other hand, for the $[1\bar{1}1]$ longitudinal waves the strength of the electron–phonon coupling in the $[\bar{1}1\bar{1}]$ valley is three times those in the other three valleys and twice that for the $[1\bar{1}0]$ longitudinal waves. Note that for case B the valley most strongly coupled with the sound waves rises in energy with increasing X (see equation (2)).

In the framework of the effective-mass approximation, a donor state in the many-valley system can be expressed by an appropriate linear combination of wavefunctions associated with each valley (Kohn 1957). Therefore, the electron–phonon coupling in such a donor state or an impurity band arising from interaction between the donors can be derived from that in the conduction band valleys. The Sb donor in Ge is assumed to be the effective-mass-like donor.

4.2. The density of states

It is a difficult problem to calculate exactly the low-lying electronic states and the density $D(E)$ of states of heavily doped semiconductors because we must treat the impurity and the conduction bands on an equal footing, taking account of randomness and electron–electron interactions. In n-type Ge and Si the many-valley structure must also be taken into account. Much theoretical work has been done on this problem (see, e.g., Perondi *et al* (1990), Mikheev (1991) and van Miegheim *et al* (1991)). At $T = 0$ K, all the low-lying states are localized for $N < N_c$, while for $N > N_c$ the localized and the extended states seem to coexist (Phillips 1983).

As we do not yet have a quantitative theory for $D(E)$, we try to obtain an empirical form for it. $D(E)$ for Sb-doped Ge can be obtained from fitting the temperature dependence of Δv without stress under the assumption that the electron–phonon coupling in the impurity band is the same as in the conduction band. In I the following simple functional form for the density $N(E)$ $(= \frac{1}{4}D(E))$ of states per valley has been assumed:

$$N(E) = AE^{1/2}\theta(E) + B\beta^{1/2}\exp[-\beta(E - E_0)^2] \tag{3}$$

where A, B, E_0 and β are adjustable parameters and $\theta(x) = 1$ $(x > 0)$ or 0 $(x < 0)$. The $\Delta v(T)$-values are calculated using equations (4)–(6) given below where all $\varphi^{(j)}$ are identical for zero stress. Only A, B, E_0 and β are changed so as to reproduce the experimental data as much as possible under the constraint that the shape of $N(E)$ becomes smoother as N increases. Some $D(E)$ have been shown in figure 6 of I for $N > 10^{17}$ cm$^{-3} \simeq 0.7N_c$.

We have carried out revised calculations of $\Delta v(T)$ using equation (3) and obtained $N(E)$ from a better fitting than in I. Figure 2 shows $N(E)$ for $N = 1.3 \times 10^{17}$, 1.8×10^{17}, 3.3×10^{17}, 4.6×10^{17} and 1.3×10^{18} cm^{-3}. The quality of fitting is also shown in the insets in figure 2 where the full curves and full circles represent the calculated curves and the experimental data, respectively. In the case when $\Delta v(T)$ weakly depends on T, there is ambiguity in determining $N(E)$. For 1.3×10^{18} cm^{-3}, $N(E)$ shown by the dotted curve has been obtained from the fitted curve represented by the broken curve in the inset. The shape of $N(E)$ changes gradually with increasing N.

It must be pointed out that the detailed shape of $N(E)$ depends on the type of electron–phonon coupling. The broken curve in figure 2(a) shows $N(E)$ for 1.3×10^{17} cm^{-3} obtained under the assumption that a fraction of localized components, 4.55×10^{15} cm^{-3}, have the same electron–phonon coupling as an isolated donor has.

$N(E)$ obtained here will be used in calculating $\Delta v(X)$ and might be useful in discussing the electrical conductivity of the Ge:Sb system at low temperatures.

4.3. The stress dependence of Δv

In calculating the stress dependence of Δv, the following assumptions are made: the shape of $N(E)$ does not vary with the stress, i.e. the impurity band associated with each valley shifts rigidly in energy according to equation (1) or equation (2) with X; the type of electron–phonon coupling does not change under the stress; strains are uniform through a sample under the external stresses. $\Delta v(X)$ can be calculated in a phenomenological way as in I or by using Green function techniques (Watanabe *et al* 1991). As the results are almost the same, we shall calculate $\Delta v(X)$ by the simpler method, namely a phenomenological technique.

For case A, $\Delta v(X)$ is given by

$$\Delta v(X) = -(4/\rho v)(\tfrac{1}{3}\Xi_u)^2[\varphi_u(\varphi_u + \varphi_d)/(3\varphi_u + \varphi_d)] \tag{4}$$

and, for case B,

$$\Delta v(X) = -(16/9\rho v)(\tfrac{1}{3}\Xi_u)^2[\varphi_u(\varphi_u + 2\varphi_d)/(\varphi_u + \varphi_d)] \tag{5}$$

where $\rho = 5.35$ g cm^{-3} is the mass density, $v = 5.45 \times 10^5$ cm s^{-1} and 5.60×10^5 cm s^{-1} are the sound velocities for case A and case B, respectively. φ_u and φ_d are the density-of-states functions for the upper and the lower valleys under the stress and are as follows. For case A,

$$\varphi_u = \varphi^{(2)} = \varphi^{(3)} = \varphi^{(4)}$$

$$\varphi_d = \varphi^{(1)}$$

and, for case B,

$$\varphi_u = \varphi^{(2)} = \varphi^{(3)}$$

$$\varphi_d = \varphi^{(1)} = \varphi^{(4)}$$

with

$$\varphi^{(j)} = -\int N^{(j)}(E)\frac{\partial f(E, \mu)}{\partial E}\, \mathrm{d}E. \tag{6}$$

Here $N^{(j)}$ is given by equation (3), f is the Fermi–Dirac distribution function and μ is the chemical potential.

Figure 3 shows the calculated $\Delta\bar{v}(X)$ $(= \Delta v(X) - \Delta v(0))$ for $N = 1.1 \times 10^{17}$, 1.3×10^{17}, 1.6×10^{17}, 1.8×10^{17}, 4.6×10^{17} and 1.3×10^{18} cm^{-3} for case A ($X\|[111]$; $q\|[1\bar{1}0]$) and case B ($X\|[110]$; $q\|[1\bar{1}1]$). The insets in figures 3(a) and 3(c) show $N(E)$ on the same scale as in figure 2 under the zero stress used in calculations. The calculations reproduce the experiment roughly, but not in detail. The stress might change the shape of $N(E)$ and also the type of electron–phonon coupling for $N \lesssim N_c$. It is necessary for a quantitative comparison to take into account the non-uniformity of the strains.

The calculated values of $\Delta\bar{v}(X)$ for 1.3×10^{18} cm^{-3} are about half the experimental values and the temperature dependence is opposite to the experiment. When the shape of $N(E)$ is parabolic or nearly parabolic, $\Delta\bar{v}(X)$ is largest at 4.2 K and smallest at 2.3 K for X up to 3×10^8 dyn cm^{-2} (not distinguishable in figure 3(e)), which is opposite to experiment. Although the discrepancy might be due to the non-uniformity of the concentration and strains and so on, we do not know the cause definitely at present. A more refined experiment and analysis are desirable.

In conclusion we have given the results of the stress dependence of the change in sound velocity in Sb-doped Ge measured over a concentration range 1.1×10^{16}–1.3×10^{18} cm^{-3} and temperature range 2.3–4.2 K. The data for 10^{17} cm$^{-3} < N < 5 \times 10^{17}$ cm^{-3} can be qualitatively explained on the basis of the density of states obtained from fitting to the temperature dependence of the change in sound velocity under zero stress.

References

Asano K, Ogiwara H and Suzuki K 1988 *J. Phys. C: Solid State Phys.* **21** 1477
Fritzsche H 1960 *Phys. Rev.* **119** 1899
—— 1962 *Phys. Rev.* **125** 1552
Keyes R W 1968 *Solid State Physics* vol 20, ed F Seitz, D Turnbull and H Ehrenreich (New York: Academic) p 37
Kohn W 1957 *Solid State Physics* vol 5, ed F Seitz and D Turnbull (New York: Academic) p 257
Kohno M, Ogiwara H, Asano K and Suzuki K 1988 *J. Phys. C: Solid State Phys.* **21** 4033
Mikheev V M 1991 *Sov. Phys.–Solid State* **33** 590
Perondi L F, Fabbi M and Ferreira da Silva A 1990 *Solid State Commun.* **73** 307
Phillips J C 1983 *Phil. Mag.* B **47** 407
Sota T and Suzuki K 1982 *J. Phys. C: Solid State Phys.* **15** 6991
Umebayashi T, Akao F and Suzuki K 1989 *Phonon 89* ed S Hunklinger, W Ludwig and G Weiss (Singapore: World Scientific) p 1199
van Miegheim P, Borghs G and Mertens R 1991 *Phys. Rev.* B **44** 12822
Watanabe H, Sota T and Suzuki K 1991 *J. Phys.: Condens. Matter* **3** 4547